Available online at www.sciencedirect.com
ScienceDirect
Journal of Hazardous Materials 154 (2008) 407–416
Journal of Hazardous Materials
www.elsevier.com/locate/jhazmat

Removal of Pb(II) from aqueous solution by oxidized multiwalled carbon nanotubes

Di Xu, Xiaoli Tan, Changlun Chen, Xiangke Wang *

Institute of Plasma Physics, Chinese Academy of Sciences, P.O. Box 1126, 230031 Hefei, China

Received 24 July 2007; received in revised form 6 September 2007; accepted 11 October 2007
Available online 23 October 2007

Abstract

Oxidized multiwalled carbon nanotubes (MWCNTs) were employed as sorbent to study the sorption characteristic of Pb(II) from aqueous solution as a function of contact time, pH, ionic strength, foreign ions, and oxidized MWCNTs' contents under ambient conditions using batch technique. The results indicate that sorption of Pb(II) on oxidized MWCNTs is strongly dependent on pH values, and independent of ionic strength and the type of foreign ions. The removal of Pb(II) to oxidized MWCNTs is rather quickly and the kinetic sorption can be described by a pseudo-second-order model very well. Sorption of Pb(II) is mainly dominated by surface complexation rather than ion exchange. The efficient removal of Pb(II) from aqueous solution is limited at pH 7–10. X-ray photoelectron spectroscopy (XPS) is performed to study the sorption mechanism at a molecular level and thereby to identify the species of the sorption processes. The 3-D relationship of pH, C_{eq} and q indicates that all the data of $C_{eq} - q$ lie in a straight line with slope $-V/m$ and intercept C_0V/m for the same initial concentration of Pb(II) and same content of oxidized MWCNTs of each experimental data.

Keywords: MWCNTs; Pb(II); Sorption; pH; Ionic strength; XPS

1. Introduction

Lead in the natural environment arises from both natural and anthropogenic sources, and is detrimental to human and living things. Long-term drinking water containing high level of lead will cause serious disorders, such as anaemia, kidney disease and mental retardation [1]. The enrichment and bioavailability of Pb(II) by plants and crops can transfer Pb(II) from natural environment to human. Metal ions are non-biodegradable, and therefore must be removed from water to eliminate the potential dangerous to human and environment. Many conventional methods have been used to remove metal ions from aqueous solutions including oxidation, reduction, precipitation, membrane filtration, ion exchange and sorption. Among the above methods, the promising process for the removal of metal ions from water and wastewater is sorption. Therefore, investigations of new promising adsorbents with high adsorption capacities and efficiencies have been the aims of many researchers [2].

Since carbon nanotubes (CNTs) were discovered by Iijima in 1991 [3], they have come under intense multidisciplinary study because of their unique physical and chemical properties and their possible applications. CNTs include single-walled carbon nanotubes (SWCNTs) and multiwalled carbon nanotubes (MWCNTs) dependent on the number of layers comprising them. Because of their structure properties with nanometer-order size and pseudo-graphite layers, MWCNTs have been expected to apply for the electrochemical storage of hydrogen [4] and a promising sorbent of heavy metal ions and radionuclides [5–8]. Although sorption of lead by carbon nanotubes and clay minerals has been studied extensively, the sorption mechanism of lead by nanotubes is still ambiguous, especially in the presence of different anion or cation ions.

In this work, the removal of lead by oxidized MWCNTs under ambient conditions will be investigated. The purposes of this work are: (1) to study the kinetic sorption of Pb(II) onto oxidized MWCNTs; (2) to investigate the influence of pH and ionic strength on the sorption of Pb(II); (3) to compare the different foreign anion and cation ions on the removal of Pb(II) from aqueous solutions to oxidized MWCNTs; (4) to compare the sorption of Pb(II) on oxidized MWCNTs and on raw MWC-

* Corresponding author.
E-mail address: xkwang@ipp.ac.cn (X. Wang).

0304-3894/$ – see front matter © 2007 Elsevier B.V. All rights reserved.
doi:10.1016/j.jhazmat.2007.10.059

NTs; and (5) to discuss the sorption mechanism of Pb(II) on oxidized MWCNTs' surfaces.

2. Experimental

2.1. Materials

All chemicals used in the experiments were purchased in analytical purity and used without any purification. MWCNTs, with outer diameter of 20–30 nm and length of about 30 μm, were prepared by using chemical vapor deposition (CVD) of acetylene in hydrogen flow at temperature of 760 °C using Ni-Fe nanoparticles as catalysts. $Fe(NO_3)_2$ and $Ni(NO_3)_2$ were treated by sol–gel process and calcinations to get FeO and NiO and then reduced by H_2 to get Fe and Ni. The as-grown MWCNTs were added into the solution of 3 M HNO_3 to remove the hemispherical caps on the nanotubes. The mixture of 3 g MWCNTs and 400 ml 3 M HNO_3 was ultrasonically stirred for 24 h. The suspension was filtrated and then rinsed with deionized water until the pH of the suspension reached about 6, and dried at 80 °C. Thus oxidized MWCNTs were calcined at 450 °C for 24 h to remove the amorphous carbon, and used in the following experiments. Using N_2-BET method, the specific surface area of the oxidized MWCNTs was found to be 197 m^2/g. The point of zero charge, pH_{ZPC}, i.e., the pH above which the total surface of the carbon nanotubes is negatively charged, was measured at pH ∼5 [9].

Analytical-grade lead nitrate was employed to prepare a stock solution containing 1000 mg/L of Pb(II), which was further diluted with deionized water to the required Pb(II) concentrations in the sorption measurements.

2.2. Sorption procedures

The sorption experiments were carried out under ambient conditions by using batch technique. The stock solutions of oxidized MWCNTs and $NaClO_4$ were added in the polyethylene test tubes and shaken for 2 days to achieve the equilibration of $NaClO_4$ with oxidized MWCNTs, then Pb(II) solution was added in the suspension to achieve the desired concentrations of Pb(II). The pH values were adjusted with negligible amount of 0.1 or 0.01 M $HClO_4$ or NaOH. The samples were gently shaken for 36 h and filtered using 0.45 μm membrane filters. The kinetic sorption data (discussed in Section 3.2) suggested that 36 h were enough to achieve the sorption equilibration. The results of Pb(II) sorption on the polyethylene test tube wall at pH 6.0 ± 0.2 indicated that little Pb(II) was adsorbed on the tube wall, which suggested that the sorption of Pb(II) on the tube wall can be negligible.

2.3. Analytical methods

The surface functional groups of oxidized MWCNTs were characterized by Fourier transform infrared spectra (FTIR). The sample for the FTIR measurement was mounted on a BrukerEQUINOX55 spectrometer (Nexus) in KBr pellet at room temperature. The morphology of oxidized MWCNTs was examined by using field emission scanning electron microscope (SEM, JEOL JSM-6700F). The information about chemical binding of Pb(II) on the surface of solids was ascertained by XPS. The XPS spectra were recorded on powders with a thermo ESCALAB 250 spectrometer using an AlK*a* monochromator source and a multidetection analyzer, under a 10^{-8} Pa residual pressure. Surface charging effects were corrected with C 1s peak at 284.6 eV as a reference.

The concentration of Pb(II) was analyzed by spectrophotometry at wavelength of 616 nm by using Pb CAP III complex. All the experimental data were the average of duplicate or triplicate determinations. The relative errors of the data were about 5%.

3. Results and discussion

3.1. Characterization of oxidized MWCNTs

Fig. 1 shows the Fourier transform infrared spectrum of oxidized MWCNTs. The FTIR spectrum of the oxidized MWCNTs exhibit main peaks at ∼600, 1400, 1650 and 3500 cm^{-1}. Previous report [10] suggested that hydroxyl (–OH), carboxyl (–COOH) and carbonyl (>C=O) present on the surfaces of oxidized MWCNTs treated with nitric acid or sulfuric acid. The peak at 1400 cm^{-1} is associated with O–H bending deformation in carbocylic acids and phenolic groups. The signature of >C=O functional groups is evident at 1650 cm^{-1} and –OH functional groups appear at 3500 cm^{-1}. These oxygen-containing functional groups present abundantly on the external and internal surfaces of oxidized MWCNTs pores, which can provide numerous chemical sorption sites and thereby increase the sorption capacity of oxidized MWCNTs [11].

Fig. 2 shows the SEM micrograph of oxidized MWCNTs samples. It is clear that the isolated oxidized MWCNTs are usually curves and have cylindrical shapes with an external diameter of 20–30 nm. The XRD pattern of oxidized MWCNTs is given in Fig. 3. The most intense peaks of oxidized MWCNTs correspond to the (0 0 2) and (1 0 0) reflections.

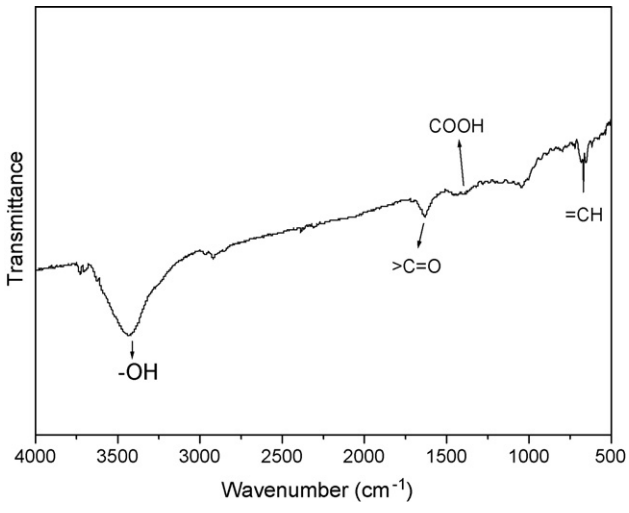

Fig. 1. Fourier transformed infrared spectra of oxidized MWCNTs.

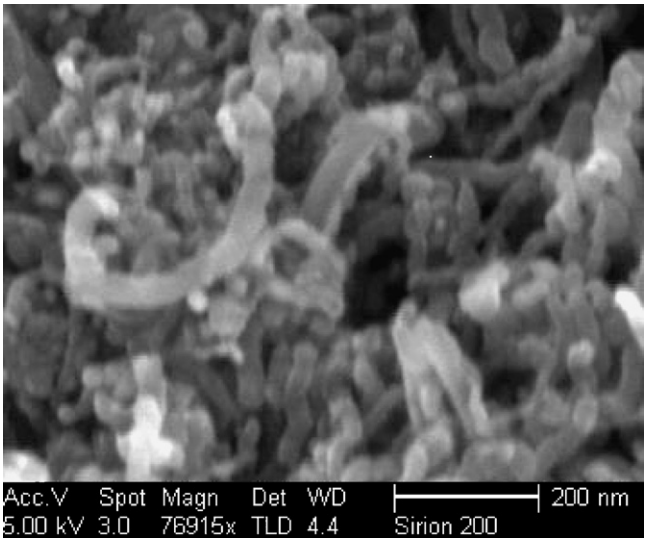

Fig. 2. Scanning electron microscope image of oxidized MWCNTs.

3.2. Sorption equilibration time

The removal of Pb(II) from aqueous solution to oxidized MWCNTs at pH 6.4 ± 0.2 as a function of contact time is shown in Fig. 4A. As can be seen from Fig. 4A, the sorption of Pb(II) on oxidized MWCNTs is very quickly and 1 h is enough to achieve the sorption equilibration. After 1 h contact time, the removal of Pb(II) from solution to oxidized MWCNTs maintains level with increasing contact time. In the following experiments, 36 h are selected to ascertain the sorption equilibrium of Pb(II) to oxidized MWCNTs. The fast sorption velocity indicate that strong chemisorption or strong surface complexation contributes to the sorption of Pb(II) on MWCNTs [5].

In order to study the specific rate constant of Pb(II)-MWCNTs system, a pseudo-second-order rate equation was used to simulate the kinetic sorption of Pb(II) on oxidized MWCNTs [9,12]:

$$\frac{t}{q_t} = \frac{1}{2K' q_e^2} + \frac{1}{q_e} t \quad (1)$$

where q_t (mg/g) is the amount of Pb(II) adsorbed on oxidized MWCNTs at time t, and q_e (mg/g) is the equilibrium adsorption capacity. K' (g mg^{-1} h^{-1}) is the pseudo-second-order rate constant of adsorption. The straight-line plots of t/q_t versus t (Fig. 4B) indicate that the kinetic sorption of Pb(II) on oxidized MWCNTs is well described by the pseudo-second-order rate equation. The values of K' and q_e are 5.24 g mg^{-1} h^{-1} and 4.09 mg g^{-1}, respectively, which are calculated from the intercept and slope of Eq. (1). The correlation coefficient of the pseudo-second-order rate equation for the linear plot is 0.9998, which suggests that the kinetic adsorption can be described by the pseudo-second-order rate equation very well. From the value of K', it also indicates the adsorption process achieves equilibration very quickly.

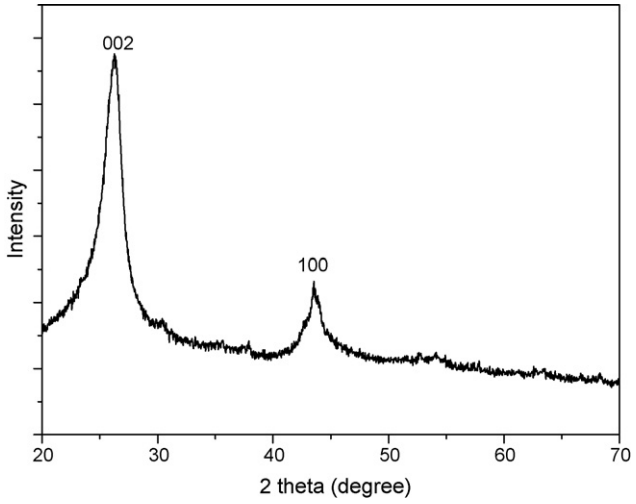

Fig. 3. XRD pattern of oxidized MWCNTs.

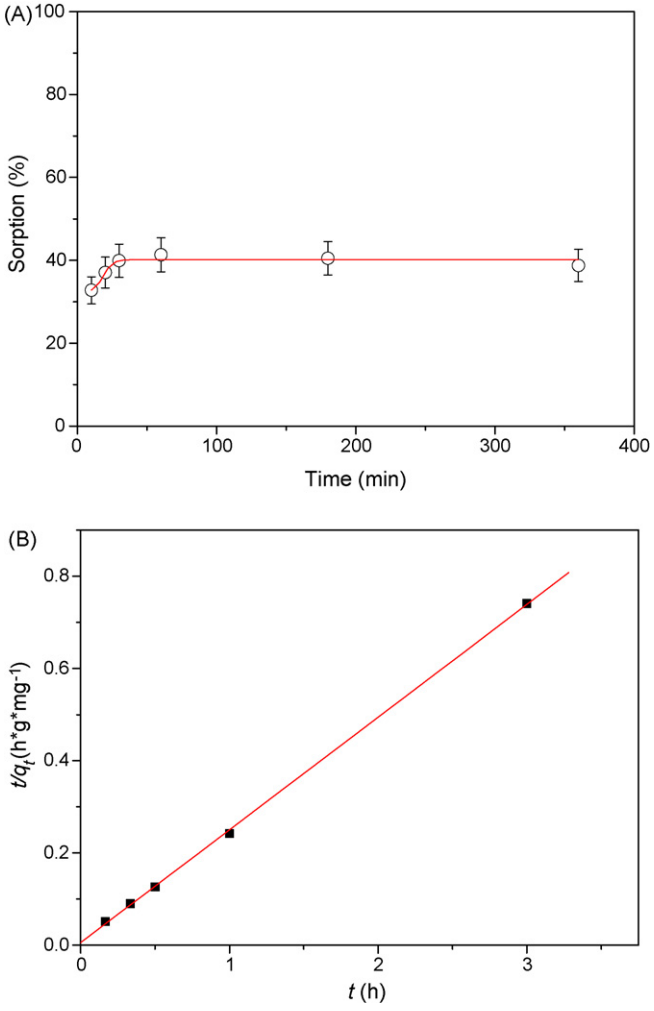

Fig. 4. (A) Effect of time on the sorption of Pb(II) to oxidized MWCNTs. $C[Pb(II)]_{initial} = 4.83 \times 10^{-5}$ mol/L, pH = 6.4 ± 0.2, I = 0.01 M $NaClO_4$, m/V = 1.0 g/L, T = 293 K. (B) Pseudo-second-order kinetic for the sorption of Pb(II) to oxidized MWCNTs. $C[Pb(II)]_{initial} = 4.83 \times 10^{-5}$ mol/L, pH = 6.4 ± 0.2, I = 0.01 M $NaClO_4$, m/V = 1.0 g/L, T = 293 K.

3.3. Effect of MWCNTs contents

Removal of Pb(II) on oxidized MWCNTs as a function of MWCNTs content is shown in Fig. 5. One can see that the removal percent of Pb(II) increases with increasing oxidized MWCNTs contents in the suspension. With increasing oxidized MWCNTs contents in the suspension, the functional sites at oxidized MWCNTs surfaces which participate in the sorption of Pb(II) increase and thereby the removal percent of Pb(II) increases reasonably. It is well known that a large amount of oxygen-containing functional groups present at the surfaces of oxidized MWCNTs. These functional groups provide binding sites to cooperate with metal ions on MWCNTs' surfaces, and these hydrophilic groups also make MWCNTs to be dispersed more easily in water. The hydrophilic groups at oxidized MWCNTs' surfaces make metal ions to contact with MWCNTs completely and thereby to be adsorbed on MWCNTs easily.

3.4. Effect of ionic strength

Influence of $NaClO_4$ concentration on the sorption of Pb(II) to oxidized MWCNTs is shown in Fig. 6. One can see that the sorption of Pb(II) on oxidized MWCNTs is independent of ionic strength in the range of 0.002–0.3 mol/L. The distribution coefficient (K_d) is calculated from the initial concentration of Pb(II) in suspension (C_0) and that of Pb(II) in supernatant (C_{eq}) after centrifugation according to the following equation:

$$K_d = \frac{C_0 - C_{eq}}{C_{eq}} \cdot \frac{V}{m} \quad (2)$$

where V is the volume of the solution and m is the mass of MWCNTs.

The ionic strength independent sorption suggests that strong inner-sphere complexes or chemical sorption are the main sorption mechanism of Pb(II) on oxidized MWCNTs [13]. It is clear that the K_d values at pH 6.4 are higher than those at pH 6.1, which suggests that sorption of Pb(II) on MWCNTs is strongly dependent on pH values. The pH dependent and ionic strength independent sorption suggest that the removal of Pb(II) from solution to oxidized MWCNTs are mainly dominated by surface complexation rather than ion exchange. Generally, the sorption mechanism of surface complexation is pH dependent, whereas ion exchange is ionic strength dependent.

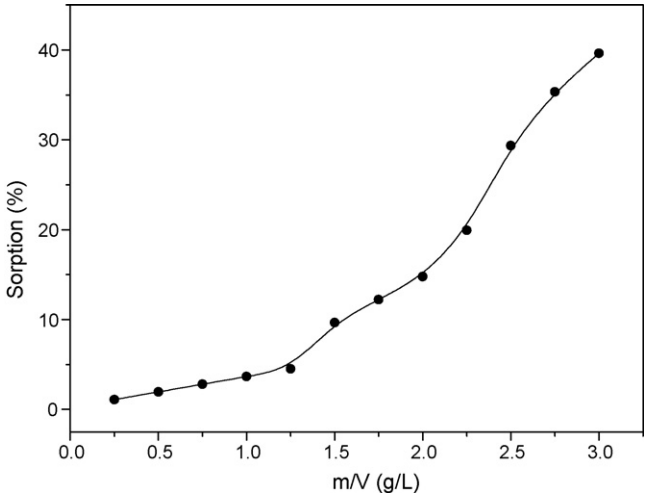

Fig. 5. Effect of sorbent content on the sorption of Pb(II) to oxidized MWCNTs. $C[Pb(II)]]_{initial} = 4.83 \times 10^{-5}$ mol/L, pH = 6.1 ± 0.1, I = 0.01 M $NaClO_4$, T = 293 K.

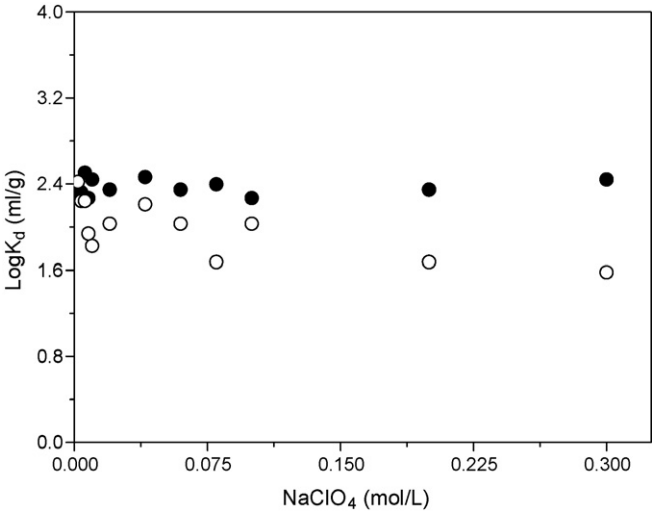

Fig. 6. Effect of ionic strength on Pb(II) sorption to oxidized MWCNTs. $C[Pb(II)]_{initial} = 4.83 \times 10^{-5}$ mol/L, m/V = 1.0 g/L, T = 293 K. Solid points: pH = 6.4 ± 0.1, open points: pH = 6.1 ± 0.1.

3.5. Effect of pH and foreign ions

Fig. 7 shows the sorption of Pb(II) on oxidized MWCNTs in the presence of 0.01 M $NaClO_4$, $KClO_4$, NaCl and $NaNO_3$, respectively, as a function of pH values. It is clear that the pH of the solution plays an important role on the sorption characteristics of Pb(II) to oxidized MWCNTs. The removal of Pb(II) increases very quickly from about 10–90% at pH 6–7, maintains level with increasing pH values at pH 7–10, and then decreases steeply at pH 10–12. It is known that lead species present in the forms of Pb^{2+}, $Pb(OH)^+$, $Pb(OH)_2{}^0$, $Pb(OH)_3{}^-$ at different

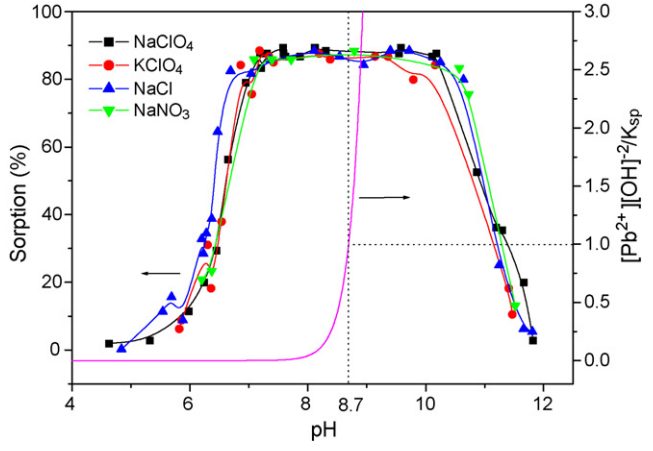

Fig. 7. Variation in sorption of Pb(II) to oxidized MWCNTs as a function of equilibrium pH and foreign ions. $C[Pb(II)]_{initial} = 4.83 \times 10^{-5}$ mol/L, m/V = 1.0 g/L, I = 0.01 M, T = 293 K, $K_{sp} = 1.2 \times 10^{-15}$.

Table 1
Equilibrium constants (log K) for Pb(II) hydrolysis reactions [28]

Equilibrium	log K (I = 0.01 M, T = 298 K)
$Pb^{2+} + OH^- = Pb(OH)^+$	6.48
$Pb(OH)^+ + OH^- = Pb(OH)_2$	11.16
$Pb(OH)_2^+ + OH^- = Pb(OH)_3^-$	14.16

pH values (Table 1 and Fig. 8). At pH < 6, the predominant lead specie is Pb^{2+} and the removal of Pb^{2+} is mainly accomplished by sorption reaction. Therefore, the low Pb^{2+} sorption that takes place at low pH can be attributed partly to the competition between H^+ and Pb^{2+} ions on the surface sites [14]. In the range of pH 7–10, the removal of Pb remains constant and reaches maximum. The main species at pH 7–10 are $Pb(OH)^+$ and $Pb(OH)_2^0$ and thus the removal of Pb is possibly accomplished by simultaneous precipitation of $Pb(OH)_2^0$ and sorption of $Pb(OH)^+$. At the pH range of 10–12, the predominant lead species are $Pb(OH)_2^0$ and $Pb(OH)_3^-$. Therefore, the decrease in Pb(II) sorption to oxidized MWCNTs at pH 10–12 can be attributed in part to competition among OH^- and $Pb(OH)_3^-$, the negative $Pb(OH)_3^-$ is difficult to be adsorbed on the negative surface charged oxidized MWCNTs at high pH values [15]. The precipitation constant of $Pb(OH)_{2(s)}$ is 1.2×10^{-15}, and the precipitation curve of lead at the concentration of 4.83×10^{-5} mol/L is also shown in Fig. 7. It is clear that lead begins to form precipitation at pH 8.7 if no lead is adsorbed on oxidized MWCNTs. However, ~90% lead is adsorbed on oxidized MWCNTs at pH 7, and thereby it is impossible to form precipitation because of the very low concentration of lead remained in solution. Therefore, the abrupt sorption of Pb(II) on oxidized MWCNTs at pH 6–7 is not attributed to the precipitation of $Pb(OH)_2$. The precipitation of $Pb(OH)_2$ does not play any role on the removal of Pb(II) from solution to oxidized MWCNTs at the whole pH ranges. The species of Pb(II) in solution at different pH values is most important for the removal of Pb(II) from aqueous solution to oxidized MWCNTs. From the results, it is clear that the best pH values of the system to remove Pb(II) from solution by using oxidized MWCNTs are 7–10.

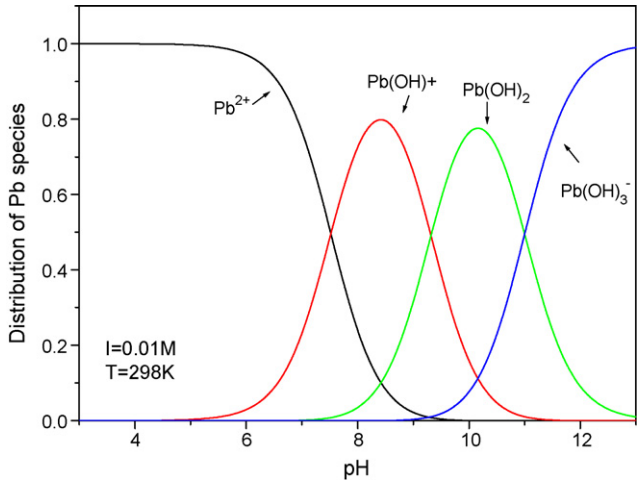

Fig. 8. Distribution of Pb(II) species as a function of pH based on the equilibrium constants.

Fig. 7 also shows that the removal of Pb(II) from aqueous solution to oxidized MWCNTs is not influenced by the background electrolyte foreign cation ions and anion ions. Cations in solution will compete for interaction with the surface functional groups of oxidized MWCNTs, and Pb(II) ions have higher affinity to the surfaces of oxidized MWCNTs than the alkali metal ions, thereby the competition of alkali ions on Pb(II) uptake to oxidized MWCNTs is almost negligible. Although the radii of hydration of K^+ = 2.32 Å and Na^+ = 2.76 Å [16] are different, the difference in the radii of hydration on the bivalent Pb(II) sorption is still very weak. The inorganic acid radicals radium order is $Cl^- < NO_3^- < ClO_4^-$, the negative charged anion ions may form complexes with the oxygen-containing functional groups on the surfaces of oxidized MWCNTs. However, the effect of Cl^-, NO_3^- and ClO_4^- on Pb(II) sorption to oxidized MWCNTs is still very weak, which suggests that surface complexes are formed on the oxidized MWCNTs surfaces. The effect of foreign ions on Pb(II) removal from solution to oxidized MWCNTs can be negligible.

The initial concentration of Pb(II) and solid oxidized MWCNTs content (i.e., m/V) are same for all experimental data. The removal of Pb(II) is different at different pH values. The amounts of Pb(II) adsorbed on solid (q) and remained in solution (C_{eq}), respectively, will change with pH changing. To illustrate the variation and relationship of pH, C_{eq}, and q, experimental data of Pb(II) sorption at pH 5–10 in 0.01 M $NaClO_4$ and in 0.01 M $KClO_4$, respectively, are plotted again as 3-D plots of pH, C_{eq}, and q (Fig. 9). It is well known that ClO_4^- does not form complexes with Pb(II) in solutions, thereby the presence of ClO_4^- on the effect of Na^+ and K^+ is negligible. On the pH–q plane, the lines are very similar to that of pH-sorption % (in Fig. 7); On the pH–C_{eq} plane, the concentration of Pb(II) remained in solution decreases with increasing pH. The projection on the pH–C_{eq} plane is just the inverted image of the projection on the pH–q plane; on the $C_{eq} - q$ plane, the projection is a straight line containing all experimental data. The slope and the intercept calculated from $C_{eq} - q$ line are −1.0 and

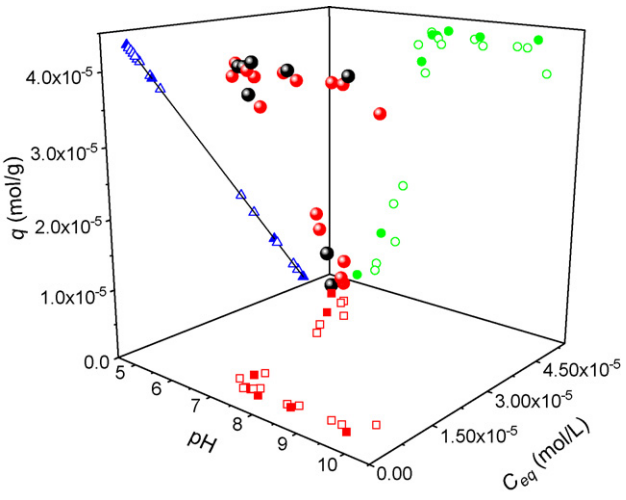

Fig. 9. 3D-plots of pH, C_{eq} and q of Pb(II) sorption to oxidized MWCNTs. $C[Pb(II)]_{initial} = 4.83 \times 10^{-5}$ mol/L, m/V = 1.0 g/L, T = 293 K. Solid points: I = 0.01 M $NaClO_4$, open points: I = 0.01 M $KClO_4$.

4.83×10^{-5}, which are quite in agreement with the values of $V/m = 1.0$ (L/g) and $C_0 V/m = 4.83 \times 10^{-5}$ (mol/g) (i.e., the values calculated from $V/m = 1.0$ L/g and $C_0 = 4.83 \times 10^{-5}$ mol/L). Thus, the complexity of the sorption edge relative to sorption isotherm is demonstrated. The 3-D plots show the relationship of pH, C_{eq}, and q very clearly, i.e., all the data of $C_{eq} - q$ lie in a straight line with slope $-V/m$ and intercept $C_0 V/m$ for the same initial concentration of Pb(II) and same solid content.

3.6. XPS investigation

In order to achieve the molecular level information of Pb(II) sorption on oxidized MWCNTs at different pH values, XPS technique are performed to identify the local structures of Pb(II) sorption on oxidized MWCNTs. Typical XPS spectra obtained after Pb(II) sorption on oxidized MWCNTs at pH 6.05 and 8.86 are shown in Fig. 10a–c. Fig. 10a shows the high resolution XPS C 1s spectra. The peak of typical graphitic carbon at 284.7 eV represents the C 1s binding energy of the MWCNTs. One can see that there is no difference in C 1s spectra of the two samples, which suggests that the species of carbon is not influenced by pH values. Fig. 10b shows the high resolution XPS O 1s spectra of the sample around 532.5 eV. With reference to the XPS studies of CNTs, the experimental data shows that functional groups present on the surface of MWCNTs: carboxyl oxygen [–O–C=O(H), 533.6 eV] and carbonyl oxygen =C=O, 530.7 eV [17]. From Fig. 10b, it can be seen that there is a significant difference between the oxygen peaks at pH 6.05 and pH 8.86. Pb(II) sorption is accompanied by a change in oxygen binding, providing evidence that the oxygen-containing functional groups on the surface of oxidized MWCNTs take part in Pb(II) sorption. The oxygen peak is shifted by 0.55 eV between pH 8.86 and 6.05. This shift may be due to that $Pb(OH)_2$ pellets begin to occur and cover the adsorbent surface at pH 8.86. The characteristic low binding energy XPS feature is present in the Pb 4*f* XPS signal at pH 6.05 and 8.86 (Fig. 10c). This XPS feature is perhaps associated with a MWCNT-OPb complex at pH 6.05 and MWCNT-$Pb(OH)_2$ pellet formation at pH 8.86. Fig. 10c shows that doublets characteristic of Pb at pH 6.05 appear at 139.0 eV (assigned to Pb $4f_{7/2}$) and at 143.85 eV (assigned to Pb $4f_{5/2}$), and doublets characteristic of Pb at pH 8.86 appear at 138.6 eV (assigned to Pb $4f_{7/2}$) and at 143.45 eV (assigned to Pb $4f_{5/2}$), respectively. The peak observed at 139.0 eV agrees with the 139.0 eV value reported for PbC_2O_4 and the peak observed at 138.6 eV agrees with the 138.4 eV value reported for $Pb(OH)_2$ [18]. This indicates further complexation of Pb onto oxidized MWCNT at pH 6.05 and precipitation of Pb occurs at high pH value.

3.7. Sorption isotherms

Three models have been adopted in this paper, namely, the Langmuir, Freundlich and D–R equilibrium isotherm models. The Langmuir and Freundlich isotherms are used most commonly to describe the sorption characteristics of sorbent in water and wastewater treatment.

The Langmuir model was first used to describe the sorption of gas molecules onto metal surface [19]. However, this model has been used successfully in many other processes. The form of Langmuir isotherm can be represented by the following equation

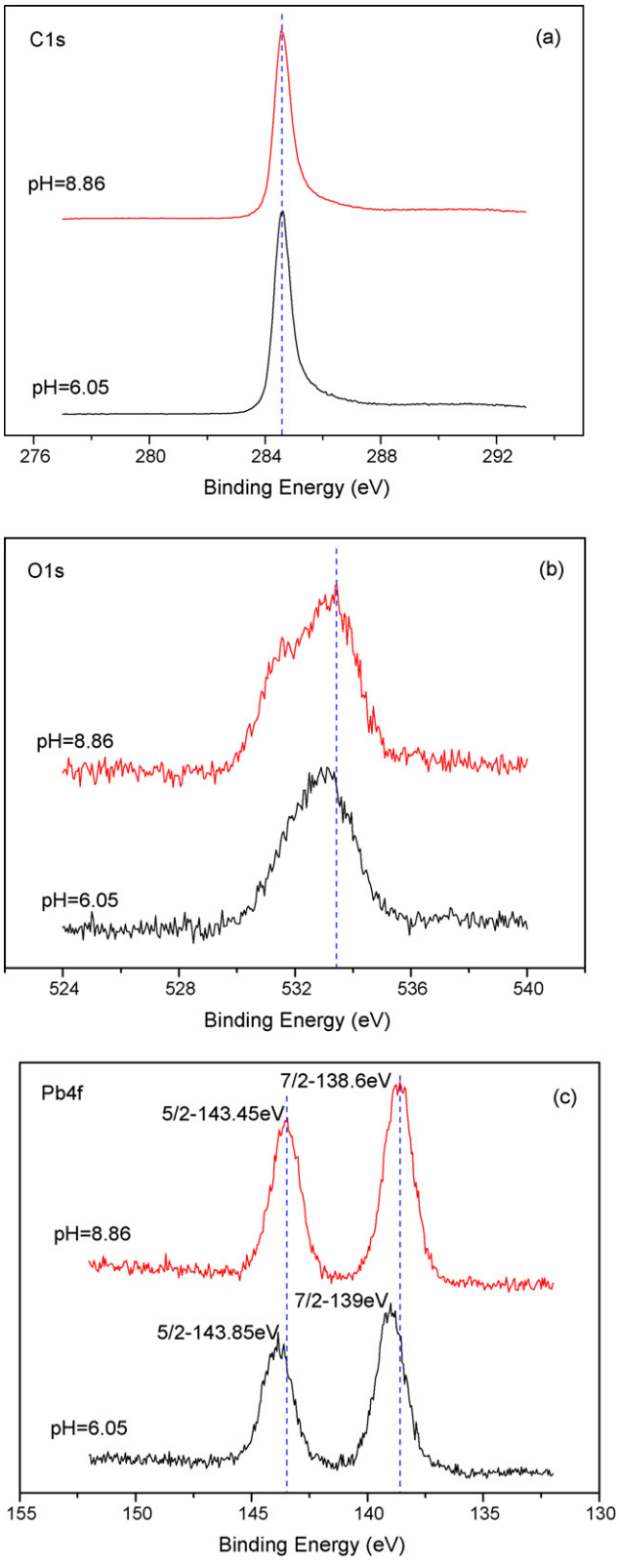

Fig. 10. XPS spectra for free-dried samples of Pb(II) adsorbed on MWCNTs. (a): C 1s; (b): O 1s; (c): Pb 4f.

[20,21]:

$$q = \frac{bq_{\max}C}{1 + bC} \tag{3}$$

Eq. (3) can be expressed in linear form:

$$\frac{C}{q} = \frac{1}{bq_{\max}} + \frac{C}{q_{\max}} \tag{4}$$

where C is the equilibrium concentration of metal ions remained in the solution (mol/L); q is the amount of metal ions sorbed on per weight unit of solid after equilibrium (mol/g); $q_{\max}$ and b are Langmuir constants related to sorption capacity and sorption energy, respectively. $q_{\max}$, the maximum sorption capacity, is the amount of sorbate at complete monolayer coverage (mol/g), and b (L/mol) is a constant that relates to the heat of sorption.

The Freundlich isotherm model stipulates that the ratio of solute adsorbed on solid surface to the solute concentration is a function of the solution concentration. This model allows for several kinds of sorption sites on the solid and represents properly the sorption data at low and intermediate concentrations on heterogeneous surfaces. The model has the following form [22,23]:

$$q = k_F C^n \tag{5}$$

Eq. (5) can be expressed in linear form:

$$\log q = \log k_F + n \log C \tag{6}$$

where k_F ($\mathrm{mol}^{1-n}\,\mathrm{L}^n/\mathrm{g}$) represents the sorption capacity when metal ion equilibrium concentration equals to 1, and n represents the degree of dependence of sorption with equilibrium concentration.

The D–R isotherm model is valid at low concentration ranges and can be used to describe sorption on both homogeneous and heterogeneous surfaces [24]. The D–R equation has the general expression:

$$q = q_{\max} \exp(-\beta\varepsilon^2) \tag{7}$$

or in the linear form:

$$\ln q = \ln q_{\max} - \beta\varepsilon^2 \tag{8}$$

where q and $q_{\max}$ are defined above, β is the activity coefficient related to mean sorption energy ($\mathrm{mol}^2/\mathrm{kJ}^2$), and ε is the Polanyi potential, which is equal to:

$$\varepsilon = RT \ln\left(\frac{1+1}{\mathrm{C}}\right) \tag{9}$$

where R is ideal gas constant ($8.3145\,\mathrm{J\,mol^{-1}\,K^{-1}}$), T is the absolute temperature (K).

Table 2
The parameters for Langmuir, Freundlich and D–R isotherms

Models	Parameters		
	b (L/mol)	$q_{\max}$ (mol/g)	R
Langmuir	1.78×10^4	9.92×10^{-6}	0.977
	k_F ($\mathrm{mol}^{1-n}\,\mathrm{L}^n/\mathrm{g}$)	n	R
Freundlich	7.57×10^{-4}	0.518	0.996
	β ($\mathrm{mol}^2/\mathrm{kJ}^2$)	$q_{\max}$ (mol/g)	R
D–R	4.34×10^{-3}	5.65×10^{-5}	0.995

Sorption isotherms of Pb(II) on oxidized MWCNTs fitted by the three models are shown in Fig. 11. The relative values calculated from the three models are listed in Table 2. Freundlich and D–R models simulate the experimental data better than Langmuir model. Some earlier studies also showed that Langmuir, Freundlich and D–R isotherms simulated the sorption data of heavy metal ions on oxides and minerals well [25,26].

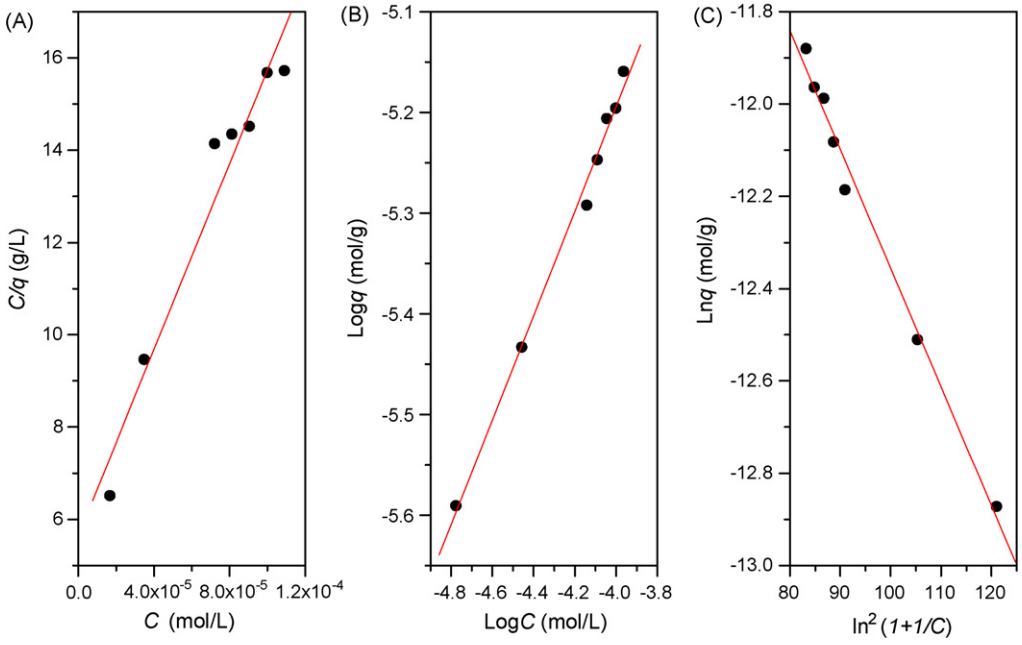

Fig. 11. Langmuir (A), Freundlich (B) and D–R (C) isotherm for Pb(II) sorption on oxidized MWCNTs. $m/V = 1.0$ g/L, pH = 5.9 ± 0.1, $I = 0.01$ M $NaClO_4$, $T = 293$ K.

The linear plot of C/q versus C with regression coefficient $R = 0.977$ is shown in Fig. 11A. From the slope of Fig. 11A, the sorption capacity of oxidized MWCNTs for Pb(II) was calculated to be 9.92×10^{-6} mol/g under the experimental conditions.

The linear plot of $\log q$ versus $\log C$ with regression coefficient $R = 0.996$ is shown in Fig. 11B. The large value of k_F indicates that the sorbent has a high sorption affinity towards metal ion. The deviation of n from unity indicates a nonlinear sorption that takes place on the heterogeneous surfaces. This behavior implies that the sorption energy barrier increases exponentially as the fraction of filled sites on the sorbent increases [27].

The linear plot of $\ln q$ versus $\ln^2(1 + 1/C)$ with regression coefficient $R = 0.995$ is shown in Fig. 11C. The values of β and q_{max} are evaluated from the slope and intercept, and found to be 4.34×10^{-3} mol^2/kJ^2 and 5.65×10^{-5} mol/g. Thus, Langmuir and D–R isotherms predict that the sorption capacity of oxidized MWCNTs for Pb(II) ion under the experimental conditions is in the range $\sim 9.92 \times 10^{-6}$–5.65×10^{-5} mol/g (i.e., 2.06–11.70 mg/g), which is consistent with the result calculated from the pseudo-second-order rate equation (i.e., 4.09 mg/g). It is necessary to note that 10–20% of Pb(II) is adsorbed to oxidized MWCNTs at pH < 6.5 (see Fig. 7). This means that oxidized MWCNTs is not suitable to remove Pb(II) at low pH values. However, 90% of Pb(II) is removed from solution to oxidized MWCNTs at pH 7–10 at C(MWCNTs) = 1.0 g/L, which indicates that the maximum sorption capacity of oxidized MWCNTs to Pb(II) is at least 5–10 times higher than that at pH < 6.5. Considering the low oxidized MWCNTs content and the high removal percent at pH 7–10, oxidized MWCNTs is considered as a suitable material for the pre-concentration of Pb(II) ions from aqueous solution at pH 7–10.

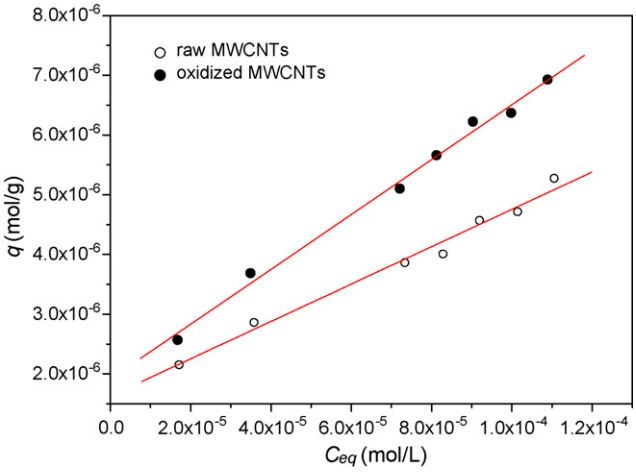

Fig. 12. Sorption isotherms of Pb(II) on the oxidized MWCNTs and on the raw MWCNTs. $m/V = 1.0$ g/L, pH = 5.9 ± 0.1, $I = 0.01$ M $NaClO_4$, $T = 293$ K.

It is well known that many oxygen-containing functional groups are produced after the raw MWCNTs is oxidized with nitric or sulfuric acids, and these functional groups are quite important in the removal of Pb(II) from solution to oxidized MWCNTs. To ascertain whether the oxygen-containing functional groups are important in binding of Pb(II) or not, sorption of Pb(II) on the raw MWCNTs is also investigated (Fig. 12). It is necessary to note that the raw MWCNTs samples are annealed in argon flow to remove its possible oxygen-containing functional groups, and then used in sorption experiments in glove box. It is clear that sorption isotherm of Pb(II) on oxidized MWCNTs is much higher than that of Pb(II) on raw MWCNTs, indicating that the sorption of Pb(II) on oxidized MWCNTs is much stronger than on raw MWCNTs. The results suggest

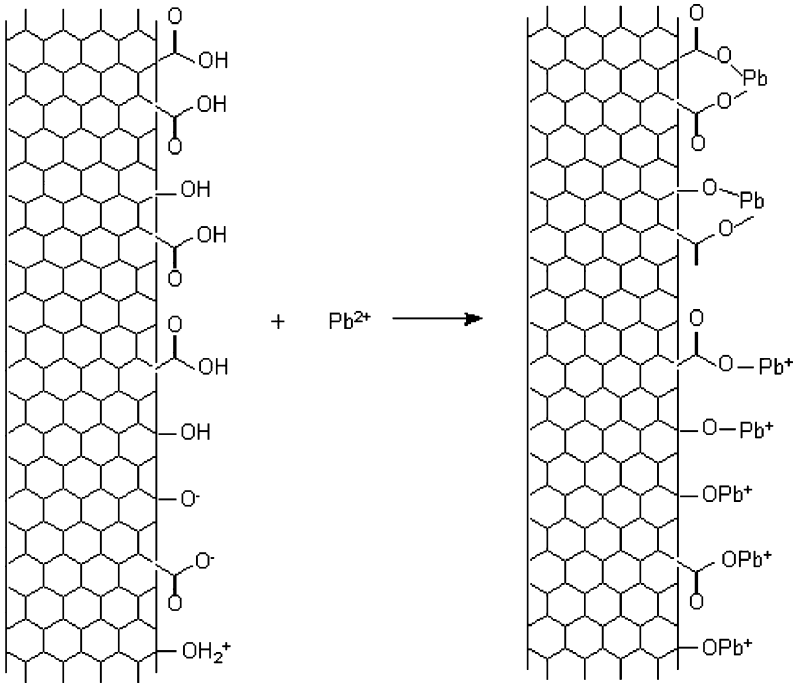

Fig. 13. Schematic diagram of the major mechanism for sorption of Pb(II) onto oxidized MWCNTs' surfaces.

that oxidized MWCNTs have higher sorption capacity than raw MWCNTs, and also ascertain that the oxygen-containing functional groups participate in the removal of Pb(II) from solution to oxidized MWCNTs. It is also interesting to notice that the sorption isotherms are linear, indicating that the sorption of Pb(II) on oxidized MWCNTs and on raw MWCNTs is far from saturation, and also suggesting that only part of the surface functional groups participate in the uptake of Pb(II) to MWCNTs.

Fig. 13 shows the schematic diagram of the major mechanisms of Pb(II) sorption to oxidized MWCNTs. The functional groups (such as $-COOH$, $-OH_2^+$, $-COO^-$, $-OH$, $-O^-$, etc) on the surfaces of oxidized MWCNTs participate in Pb(II) binding to MWCNTs. Although the oxygen-containing functional groups are dependent on pH values, the groups are enough to provide sorption sites for Pb(II) uptake from solution to oxidized MWCNTs. With increasing contact time of Pb(II) with MWCNTs, part of Pb(II) may enter to the inner channel of oxidized MWCNTs to form irreversible sorption fractions [5]. The radii of Pb(II) is much smaller than the inner-diameter of oxidized MWCNTs, it is possible for Pb(II) to enter the inner channel of oxidized MWCNTs. The velocity of Pb(II) to enter the inner channel of oxidized MWCNTs is much slower than that of Pb(II) to adsorb on the surface of oxidized MWCNTs [29]. The part of metal ions adsorbed in the inner channel of oxidized MWCNTs is ignored in the previous papers about metal ions' sorption to carbon nanotubes. This aspect should be taken into account in future works.

4. Conclusions

From the results of Pb(II) sorption on oxidized MWCNTs under our experimental conditions, the following conclusions can be obtained:

1. The sorption of Pb(II) on oxidized MWCNTs achieves the sorption equilibration rapidly. The kinetic sorption of Pb(II) on oxidized MWCNTs can be described by a pseudo-second-order model well.
2. Sorption of Pb(II) on oxidized MWCNTs is strongly dependent on pH values but independent of ionic strength and foreign ions.
3. Chemisorption and/or chemical complexation rather than cation exchange/physical sorption are the main sorption mechanisms.
4. The experimental data of Pb(II) on oxidized MWCNTs follows the Langmuir, Freundlich and D–R sorption isotherms.
5. Oxidized MWCNTs is a promising candidate for preconcentration of Pb(II) ions from large volume of solutions at pH 7–10.
6. The 3-D relationship of pH, C_{eq} and q indicates that all the data of $C_{eq} - q$ lie in a straight line with slope $-V/m$ and intercept $C_0 V/m$.

Acknowledgements

The authors acknowledge financial support from National Natural Science Foundation of China (20501019, 20677058), Ministry of Science and Technology of China (2007CB936602) and Century Project of Chinese Academy of Sciences.

References

[1] Y.H. Li, S. Wang, J. Wei, X. Zhang, C. Xu, Z. Luan, D. Wu, B. Wei, Lead adsorption on carbon nanotubes, Chem. Phys. Lett. 357 (2002) 263–266.
[2] G.P. Rao, C. Lu, F. Su, Sorption of divalent metal ions from aqueous solution by carbon nanotubes: a review, Sep. Purif. Technol. 58 (2007) 224–231.
[3] S. Iijima, Helical microtubes of graphitic carbon, Nature 354 (1991) 56–58.
[4] E. Frackowiak, F. Bguin, Electrochemical storage of energy in carbon nanotubes and nanostructured carbons, Carbon 40 (2002) 1775–1787.
[5] X.K. Wang, C.L. Chen, W.P. Hu, A.P. Ding, D. Xu, X. Zhou, Sorption of ^{234}Am(III) to multiwall carbon nanotubes, Environ. Sci. Technol. 39 (2005) 2856–2860.
[6] K. Lin, Y. Xu, G. He, X. Wang, The kinetic and thermodynamic analysis of Li ion in multi-walled carbon nanotubes, Mater. Chem. Phys. 99 (2006) 190–196.
[7] C. Chen, X. Li, D. Zhao, X. Tan, X. Wang, Adsorption kinetic, thermodynamic and desorption studies of Th(IV) on oxidized multi-wall carbon nanotubes, Colloid Surf. A: Physicochem. Eng. Asp. 302 (2007) 449–454.
[8] M. Tuzen, M. Soylak, Multiwalled carbon nanotubes for speciation of chromium in environmental samples, J. Hazard. Mater. 147 (2007) 219–225.
[9] C.L. Chen, X.K. Wang, Adsorption of Ni(II) from aqueous solution using oxidized multi-walled carbon nanotubes, Ind. Eng. Chem. Res. 45 (2006) 9144–9149.
[10] Y.H. Li, B. Xu, X. Wei, X. Zhang, M. Zheng, D. Wu, P.M. Ajayan, Self organized ribbons of aligned carbon nanotubes, Chem. Mater. 14 (2002) 483–485.
[11] C. Lu, Y.L. Chung, K.F. Chang, Adsorption thermodynamic and kinetic studies of trihalomethanes on multiwalled carbon namotubes, J. Hazard. Mater. 138 (2006) 304–310.
[12] Y.S. Ho, D.A.J. Wase, C.F. Forster, Kinetic studies of competitive heavy metal adsorption by sphagnum moss peat, Environ. Technol. 17 (1996) 71–77.
[13] X. Wang, D. Xu, L. Chen, X. Tan, X. Zhou, A. Ren, C. Chen, Sorption and complexation of Eu(II) on alumina: effects of pH, ionic strength, humic acid and chelating resin on kinetic dissociation study, Appl. Radiat. Isot. 64 (2006) 414–421.
[14] C.H. Weng, C.P. Huang, Adsorption characteristics of Zn(II) from dilute aqueous solution by fly ash, Colloid Surf. A: Physicochem. Eng. Asp. 247 (2004) 137–143.
[15] C. Lu, H. Chiu, Adsorption of zinc(II) from water with purified carbon nanotubes, Chem. Eng. Sci. 61 (2006) 1138–1145.
[16] F. Esmadi, J. Simm, Sorption of cobalt(II) by amorphous ferric hydroxide, Colloid Surf. A: Physicochem. Eng. Asp. 104 (1995) 265–270.
[17] A.M. Bond, W. Miao, C.L. Raston, Mercury(II) immobilized on carbon nanotubes: Synthesis, characterization and redo properties, Langmuir 16 (2000) 6004–6012.
[18] S. Lee, J.A. Dyer, D.L. Sparks, N.C. Scrivner, E.J. Elzinga, A multi-scale assessment of Pb(II) sorption on dolomite, J. Colloid Interface Sci. 298 (2006) 20–30.
[19] I. Langmuir, The adsorption of gases on plane surface of glass, mica and platinium, J. Am. Chem. Soc. 40 (1918) 1361–1403.
[20] Metcalf, Eddy, Inc., Wastewater Engineering: Treatment, Disposal and Reuse, third ed., Irwin/McGraw-Hill, Boston, MA, 1991.
[21] S. Chegrouche, A. Mellah, S. Telmoune, Removal of lanthanum from aqueous solutions by natural bentonite, Water Res. 31 (1997) 1733–1737.
[22] S.J. Allen, P.A. Brown, Isotherm analysis for single component and multi-component metal sorption onto lignite, J. Chem. Tech. Biotechnol. 62 (1995) 17–24.
[23] A.G. Sanchez, E.A. Ayuso, O.J. De Blas, Sorption of heavy metal from industrial waste water by low-cost mineral silicates, Clay Miner. 34 (1999) 469–477.
[24] T. Shahwan, H.N. Erten, Temperature effects in barium sorption on natural kaolinite and chlorite-illite, J. Radioanal. Nucl. Chem. 260 (2004) 43–48.

[25] P.N. Pathak, G.R. Choppin, Kinetic and thermodynamic studies of cesium(I) sorption on hydrous silica, J. Radioanal. Nucl. Chem. 270 (2006) 299–305.
[26] X.L. Tan, X.K. Wang, M. Fang, C.L. Chen, Sorption and desorption of Th(IV) on nanoparticles of anatase studied by batch and spectroscopy methods, Colloid Surf. A: Physicochem. Eng. Asp. 296 (2007) 109–116.
[27] T. Shahwan, H.N. Erten, Thermodynamic parameters of Cs^+ sorption on natural clays, J. Radioanal. Nucl. Chem. 253 (2002) 115–120.
[28] C.H. Weng, Modeling Pb(II) adsorption onto sandy loam soil, J. Colloid Interface Sci. 272 (2004) 262–270.
[29] G. Hummer, J.C. Rasaiah, J.P. Noworyta, Water conduction through the hydrophobic channel of a carbon nanotube, Nature (London) 414 (2001) 188–190.